**BJR**

■ **KNEE**

# Knee immobilization reproduces key arthrofibrotic phenotypes in mice

L. Dagneaux,
A. K. Limberg,
A. R. Owen,
J. W. Bettencourt,
A. Dudakovic,
B. Bayram,
N. M. Gades,
J. Sanchez-Sotelo,
D. J. Berry,
A. van Wijnen,
M. E. Morrey,
M. P. Abdel

*From The Mayo Clinic, Rochester, Minnesota, USA*

## Aims

As has been shown in larger animal models, knee immobilization can lead to arthrofibrotic phenotypes. Our study included 168 C57BL/6J female mice, with 24 serving as controls, and 144 undergoing a knee procedure to induce a contracture without osteoarthritis (OA).

## Methods

Experimental knees were immobilized for either four weeks (72 mice) or eight weeks (72 mice), followed by a remobilization period of zero weeks (24 mice), two weeks (24 mice), or four weeks (24 mice) after suture removal. Half of the experimental knees also received an intra-articular injury. Biomechanical data were collected to measure passive extension angle (PEA). Histological data measuring area and thickness of posterior and anterior knee capsules were collected from knee sections.

## Results

Experimental knees immobilized for four weeks demonstrated mean PEAs of 141°, 72°, and 79° after zero, two, and four weeks of remobilization (n = 6 per group), respectively. Experimental knees demonstrated reduced PEAs after two weeks ($p < 0.001$) and four weeks ($p < 0.0001$) of remobilization compared to controls. Following eight weeks of immobilization, experimental knees exhibited mean PEAs of 82°, 73°, and 72° after zero, two, and four weeks of remobilization, respectively. Histological analysis demonstrated no cartilage degeneration. Similar trends in biomechanical and histological properties were observed when intra-articular violation was introduced.

## Conclusion

This study established a novel mouse model of robust knee contracture without evidence of OA. This was appreciated consistently after eight weeks of immobilization and was irrespective of length of remobilization. As such, this arthrofibrotic model provides opportunities to investigate molecular pathways and therapeutic strategies.

Cite this article: *Bone Joint Res* 2023;12(1):58–71.

**Keywords:** Fibrosis, Genetic predisposition, Contracture, Murine

## Article focus
- Can we induce a knee contracture in mice?
- What is the ideal timeline for immobilization and remobilization for this model?
- Does the contracture resolve with remobilization?

## Key messages
- Using the surgical technique described, we can induce a knee contracture in mice with immobilization.
- The contracture was most pronounced after eight weeks of immobilization irrespective of remobilization time.
- This model preserved the knee cartilage.

## Strengths and limitations
- This technique is non-invasive, reproducible, and successfully induced a contracture in mice.
- This procedure can be employed in future studies for examining molecular pathways and potential therapeutics for arthrofibrosis.

Correspondence should be sent to Matthew P. Abdel; email: abdel.matthew@mayo.edu

■ A limitation of this study is it only used female mice.

## Introduction

Arthrofibrosis after total knee arthroplasty (TKA) is estimated to affect 4% of primary TKAs, resulting in restricted knee range of motion, pain, and dysfunction.[1] As such, arthrofibrosis is associated with decreased patient satisfaction and high rates of reoperation and revision.[1,2] Despite the devastating impact arthrofibrosis has on patients, pharmacological methods that prevent and/ or treat this pathological process are lacking.[2] Animal models which permit examination of the fundamental mechanisms that promote arthrofibrosis may provide insights into the development of therapeutic interventions for this debilitating disease.[3]

In the current literature, there are previously developed and validated animal models of arthrofibrosis in the rabbit[4-6] and in the rat.[7] The rabbit model has been used to demonstrate that pharmacological interventions, including celecoxib, subcutaneous ketotifen injection, and rosiglitazone-loaded hydrogels, can be employed to reduce the severity of arthrofibrosis in vivo.[8–12] However, rabbits are costly, and limitations in genetic options (e.g. gene knockout models) present barriers to understanding gene-specific contributions to arthrofibrosis. Conversely, mice are optimal for such investigations given the relatively low cost associated with their use and full array of genetic options, specialized strains, and maintenance protocols. The latter versatility permits examination of the biological effects on gene loss of function and potential comorbidities (e.g. diabetes and metabolic disease models). Yet, there are no current mouse models of arthrofibrosis that do not involve initial or concurrent development of osteoarthritis (OA). Current dual models of OA and arthrofibrosis are induced by joint destabilization, cartilage resection, and administration of biologics within the joint (e.g. transforming growth factor β1),[13–15] or a combination of approaches.[16–18] OA and arthrofibrosis share common biomolecular mechanisms of pathogenesis.[13] Therefore, an arthrofibrosis model that does not involve cartilage specific pathways is critical to understanding the fibrotic cascade governing the pathogenesis of arthrofibrosis. As such, the objective of this study was to establish a persistent arthrofibrotic phenotype in mice, including changes in biomechanical and histological parameters, which does not involve cartilage damage, using a minimally disruptive surgical technique.

## Methods

**Ethical treatment of animals.** All experiments were conducted in accordance with the Guide for the Care and Use of Laboratory Animals (2011).[19] Experiments were approved by the Institutional Animal Care and Use Committee of the Mayo Clinic (IACUC # A00004221), the protocol being prepared and registered before the study. All animal experiments were approved and monitored by the veterinary staff at our institution, and all experiments adhered to the ARRIVE guidelines.

**Strain maintenance.** Mice were socially housed (6/cage) in 1,800 cm$^2$ polysulfone cages (Allentown, USA). Mice were monitored twice daily and were provided with cage enrichment resources. The mouse diet consisted of a commercially supplied pelleted chow, PicoLab Rodent Diet 20 (USA), and filtered tap water ad libitum. Mice were housed at a constant room temperature (23°C) with 12 hours of light exposure daily.

**Study design.** A total of 168 12-week-old C57BL/6 J female mice were used in our study (Envigo, USA). The mean weight at the time of surgical procedure was 22 g (19 to 26). Of the 168 mice, 24 served as controls (randomly assigned, no surgical intervention) while 144 mice underwent an experimental knee procedure (right knee). Mice were killed and limbs were harvested at various timepoints (Figure 1).

The 144 experimental mice were randomly divided into two groups of 72 mice (Figure 1). In the first group, the right knee underwent an experimental surgical procedure (described below) and was considered the experimental limb, whereas the left contralateral knee served as an internal and a secondary control. In the second group, the same surgical procedure was completed, with the additional creation of an intra-articular lesion. The lesion was generated in a controlled fashion using an 18-gauge needle to create intra-articular but extracartilaginous lesions, in the medial and lateral femoral condyles, to promote formation of an intra-articular haematoma.

In each group of 72 animals, 36 mice were immobilized for four weeks, and 36 mice were immobilized for eight weeks. Each group of 36 animals were then remobilized for zero weeks (12 mice), two weeks (12 mice), or four weeks (12 mice) following suture removal and prior to kill (see below). In each subgroup of 12 mice, six mice were used for biomechanical testing and six mice for histopathological analysis (Figure 1). In addition, four control mice were sacrificed at the matching timepoints (one hind limb for biomechanical and the other hind limb for histology). Timepoints were chosen based upon current literature.[13,20–24]

**Surgical procedures.** All surgical procedures were conducted by a surgeon (LD), who was blinded to the endpoint of the animals, under general anaesthesia via inhalation of isoflurane (1% to 2% in oxygen) administered via a nosecone. Cefazolin (30 mg/kg) and buprenorphine SR (0.6 mg/kg) were injected subcutaneously prior to surgical incision for antibiotic prophylaxis and postoperative analgesia, respectively. The animals were prepared for surgery with povidone-iodine solution and draped in sterile fashion.

A percutaneous fixation procedure was performed on the right knee in all 144 experimental animals (Figure 2). A 21-gauge needle was used to percutaneously shuttle a nonabsorbable suture (3-0 Ethilon suture; Ethicon, Johnson & Johnson, USA). First, the needle was introduced along the anterior femur at the mid-shaft. The needle was then passed lateral to the femur and tibia to emerge on the anterior surface of the tibia. A suture was passed in
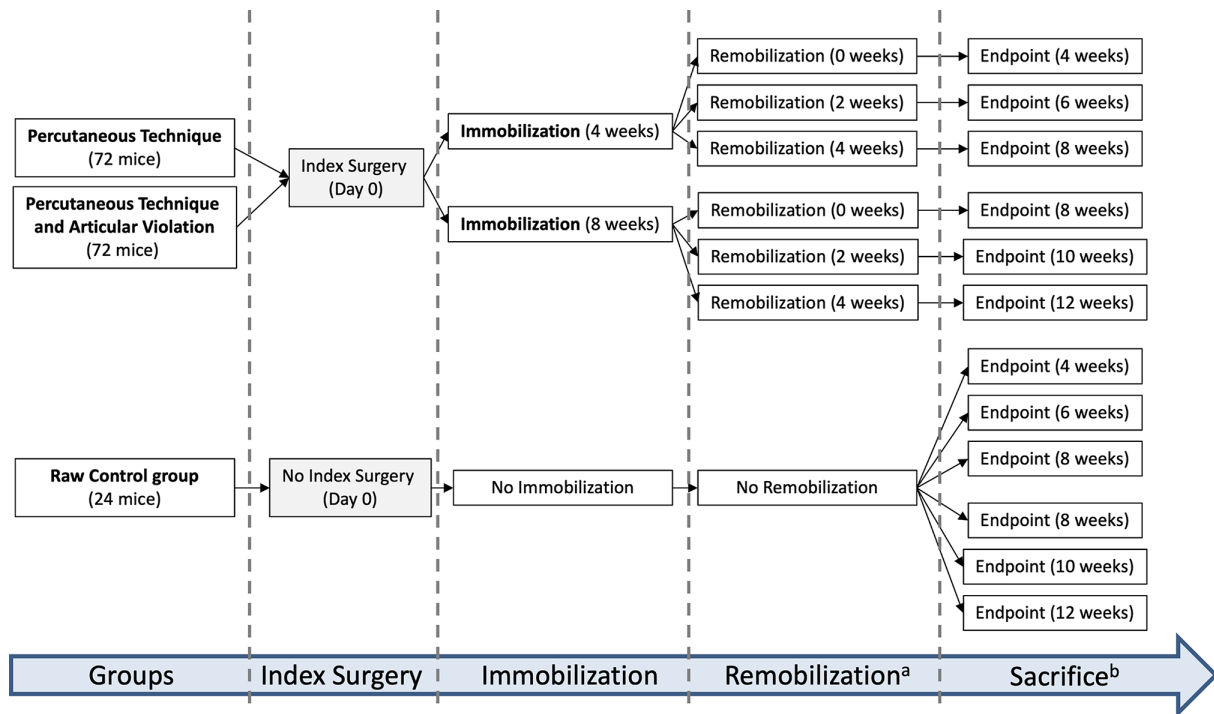
**Fig. 1**

Overall study design of novel arthrofibrosis mouse model. Study design and experimental timeline illustrating the cohort of 168 mice which were included in the percutaneous technique group (72 mice), the percutaneous and intra-articular violation technique group (72 mice), and the control group (24 mice). All the experimental subgroups contained 12 mice at each endpoint and all the control subgroups contained four mice; 50% of the lower limbs were allocated to biomechanical measurements and 50% to the histopathological assessment. [a]Remobilization period started after surgical suture removal. [b]Endpoint was defined as the duration between the index surgery and the sacrifice procedure.
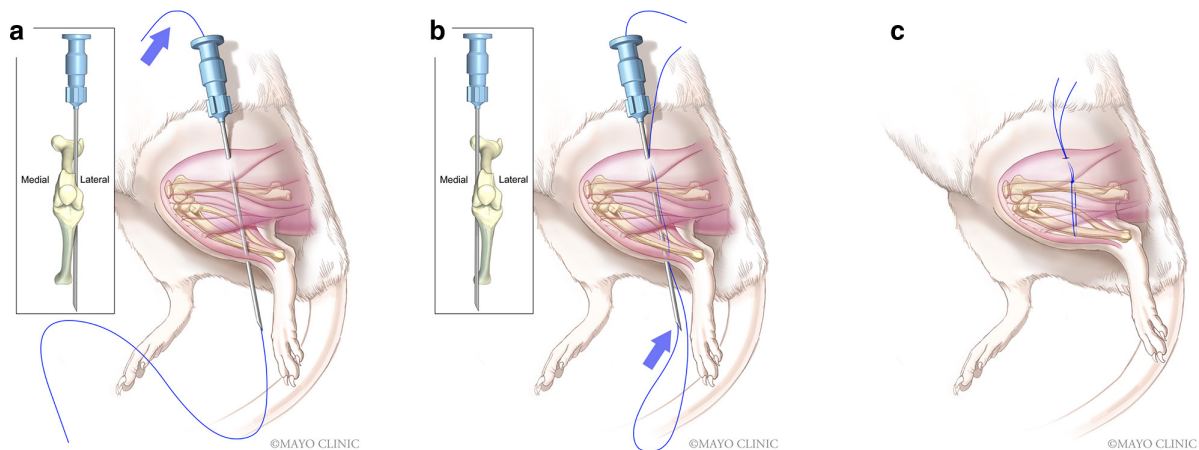


**Fig. 2**

Percutaneous fixation technique used in novel arthrofibrosis mouse model. a) A 21-gauge needle was introduced laterally to the lower limb through a lateral portal between the proximal femur and the distal tibia and a 3-0 nonabsorbable suture was shuttled using the needle. b) After removal, the same needle was introduced through the same lateral portal but medially to the femur, resulting in the creation of a loop with the suture. c) A sliding knot was used to tighten and fix the knee joint at 150° of flexion. The wound was closed and the knot was placed under the skin at the lateral part of the thigh.

retrograde fashion so that an end was shuttled to the medial aspect of the femur. The suture was looped over the anterior tibia next to the bone. Then, an arthroscopic-style Duncan loop knot was tied to secure the knee joint in approximately 150° of flexion (Figure 2).[25] Intra-articular violation was performed percutaneously in half of the experimental cohorts (72 mice) using an 18-gauge needle by perforating the medial and lateral femoral condyles. Creation of cortical defects was confirmed by observing bleeding through the femoral condyle portals. The intra-articular violation was performed to induce an intra-articular haematoma. Skin portals were closed

**Fig. 3**

A mouse limb mounted on our biomechanical testing device, adapted for the mouse model.

with absorbable suture (4-0 Vicryl, Ethicon, Johnson & Johnson) and local antibiotic ointment was applied on the portals at the end of the surgical procedure.

**Suture removal procedure.** Following the assigned period of immobilization (i.e. four weeks or eight weeks), a second procedure was performed on the experimental limbs to remove the nonabsorbable sutures prior to the remobilization period. Procedural preparation and anaesthesia were identical to those described above. A lateral thigh incision was performed at the site of the previous lateral incision and dissection carried down to the suture. The knot was cut using microsurgical scissors, the suture removed, and skin closed with absorbable suture (4-0 Vicryl, Ethicon, Johnson & Johnson). Following suture removal, animals were allowed to freely walk until time of sacrifice. Of note, we did observe some callus formation over the suture at the suture-femur interface, however

this phenomenon was not seen at the suture-tibia interface. This is likely due to the force of the animal trying to extend its limb and gravitational forces applied to the femur.

**Biomechanical testing.** A biomechanical testing device previously validated for a rabbit model of arthrofibrosis was modified to accommodate the mouse limbs (Figure 3).[26] In each group, the experimental and contralateral limbs of the six mice dedicated for biomechanical analysis were disarticulated at the hip and midfoot joints. Skin and subcutaneous tissues were removed and the proximal third of the femur was denuded of any muscular attachments. The proximal segment was then potted in a 1 cm polyvinyl chloride tube with polymethylmethacrylate (PMMA) bone cement (Stryker, USA) and mounted to a metal bracket affixed to the measuring device. Once mounted, a passive extension motion (from 135° of knee flexion to -90° of hyper-extension) was induced by the device to the harvested lower limb at a constant speed of 1°/second. During this motion, a dynamic low-capacity reaction torque sensor, which was specifically dedicated to detecting torque changes in smaller animals (RTS-25 model; Transducer Techniques, USA), registered the torque applied to the knee joint until the failure point (defined as the rupture of femoral or tibial physis or joint disruption). Data obtained from the measurement device were transformed into graphs of passive extension versus torque using Mathlab 2016a by a blinded observer (AKL) (Mathworks, USA). The passive extension angle at a single specific torque (i.e. 0.4 N-cm) was collected for all knees tested.

**Histological processing and evaluation.** For mice dedicated for histological analysis, the hind limbs were disarticulated at the hip and ankle, retaining a minimum of 1 cm of femur and tibia. The specimens were immediately immersed in 40 ml of 10% neutral buffered formalin (NBF), stored at room temperature (22°C) for 72 hours, and sent to Premier Laboratory (USA) for processing, sectioning, staining, and whole-slide scanning. Knees were decalcified in 10% formic acid for seven days, then processed to paraffin. The knees were embedded and sectioned at 5 μm intervals in the sagittal plane to capture the central sections of the knee joint. Sections were validated by two observers (LD and AKL) according to anatomical criteria previously defined to ensure the reliability of the sectioning (cruciate ligaments and/or tibial spines seen in the section). Medial, central, and lateral knee sections were identified using visualization of two triangles of the medial meniscus, ACL and/or PCL, and the fibular head as the anatomical criteria, respectively.

All sections were stained using haematoxylin and eosin (H&E), Masson's trichrome, and toluidine blue using standard methods. Stained slides were scanned at 20× magnification on Aperio ScanScope AT2 (Leica Biosystems, USA) and histological assessment was performed by two blinded observers (LD and AKL). Thickness and areas were collected from the anterior (infrapatellar fat pad) and posterior (posterior capsule) regions of the knee
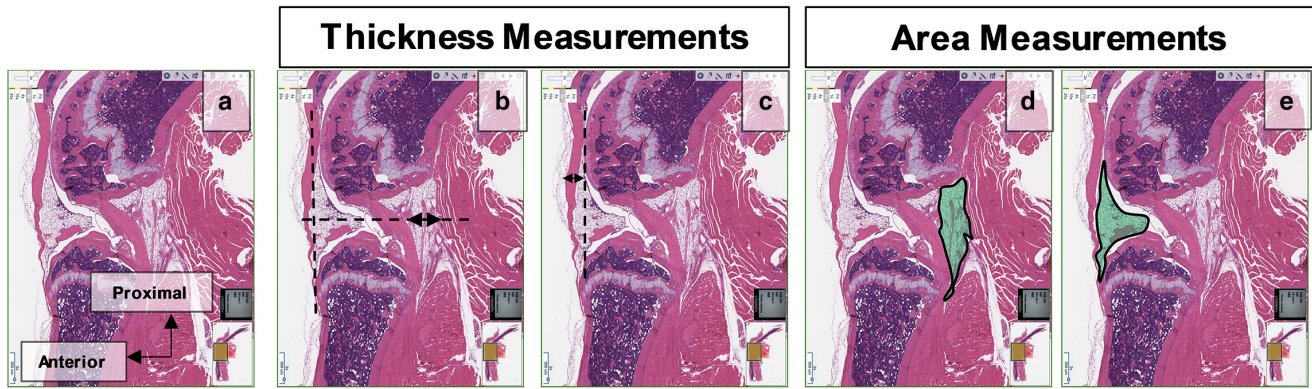
## Thickness Measurements

## Area Measurements



**Fig. 4**

Histological assessment of novel arthrofibrosis mouse model. The pictures shown summarize histological methods and measurements that were used to assess knee joints in the present study. a) A central section of a control mouse knee after haematoxylin and eosin staining. b) Measurement of the posterior capsule thickness using a line perpendicular to the patellar tendon axis. c) Measurement of the patellar tendon thickness at mid-distance between the apex of the patella and the anterior tibial tuberosity. d) The area of the posterior capsule was measured by manual contouring. e) The area of the Hoffa fat pad was measured by manual contouring.

**Table I.** Histology grading criteria for cartilage evaluation performed on the toluidine blue stained images.

| Score | Loss of cartilage matrix | Description of cartilage surface |
|---|---|---|
| 0 | Normal | Diffuse staining of superficial articular cartilage on distal femur and proximal tibia |
| 1 | Minimal | Focal loss of articular cartilage staining (usually caudal margin of femoral condyle); ≤ 10% |
| 2 | Mild | Multifocal loss of articular cartilage staining (femur and tibia); 15% to 30% |
| 3 | Moderate | Multifocal extensive loss of articular cartilage staining (femur and tibia); 35% to 55% |
| 4 | Marked | Multifocal extensive loss of articular cartilage staining (femur and tibia); 60% to 85% |
| 5 | Severe | Diffuse loss of articular cartilage staining (femur and tibia); ≥ 85% |

**Table II.** Histology grading criteria for fibrosis and fatty infiltrate.

| Score | Fibrosis description | Fatty infiltrate description |
|---|---|---|
| 0 | 0 | 0 |
| 1 | Narrow band | Minimal amount of fat associated with fibrosis |
| 2 | Moderately thick band | Several layers of fat and fibrosis |
| 3 | Thick band | Elongated and broad accumulation of fat cells about the implant site |
| 4 | Extensive band | Extensive fat completely surrounding the implant |

using Imagescope software (Leica Biosystems) after H&E staining, on the central sagittal plane sections (Figure 4). The thickness of the posterior capsule and anterior infrapatellar fat pad was evaluated using the method described by Watanabe et al.[27] Thickness measures included posterior capsule thickness along a line perpendicular to the patellar tendon, and the patellar tendon thickness at mid-distance between the patellar apex and the anterior tibial tuberosity.[27] From the central sagittal section, area measurements of the posterior capsular tissue and the Hoffa fat pad were determined by manual contouring and selection (defining the total area in square microns).

A dedicated filter was applied on this area using Aperio positive pixel count algorithm (Leica Biosystems) to quantify the real amount of stain (i.e. fibrotic tissue) and to eliminate fat and processing artifact areas (defining the fibrotic area). The ratio between the two areas was also recorded. Additionally, we quantified the fibrotic and fatty cells, and whether or not degenerative process of the femoral cartilage was present in each section, by an independent veterinary pathologist (NMG) using a previously published histopathological grading scale and toluidine blue staining (Table I, Table II).[10–12]

**Statistical analysis.** To determine the number of animals needed per group, a power analysis was performed assuming a 5% type 1 error and 80% power to detect an effect difference of 10° with a standard deviation (SD) of 8°; a minimum of six limbs was required. Therefore, for our studies six limbs were assigned to each group for the biomechanical and histological analyses. Quantitative variables were reported as means and SDs. For all experimental data, Kolmogorov-Smirnov normality tests were conducted, and either parametric or non-parametric comparisons between each treatment group and its respective control group were carried out using either independent-samples $t$-test or Mann-Whitney U test. Reliability assessment was conducted for the three histological measurements using interclass and intraclass correlation coefficients (ICCs).[28] To compute the ICCs, histological measures were performed by two independent observers (LD and AKL) for all sections and repeated by a
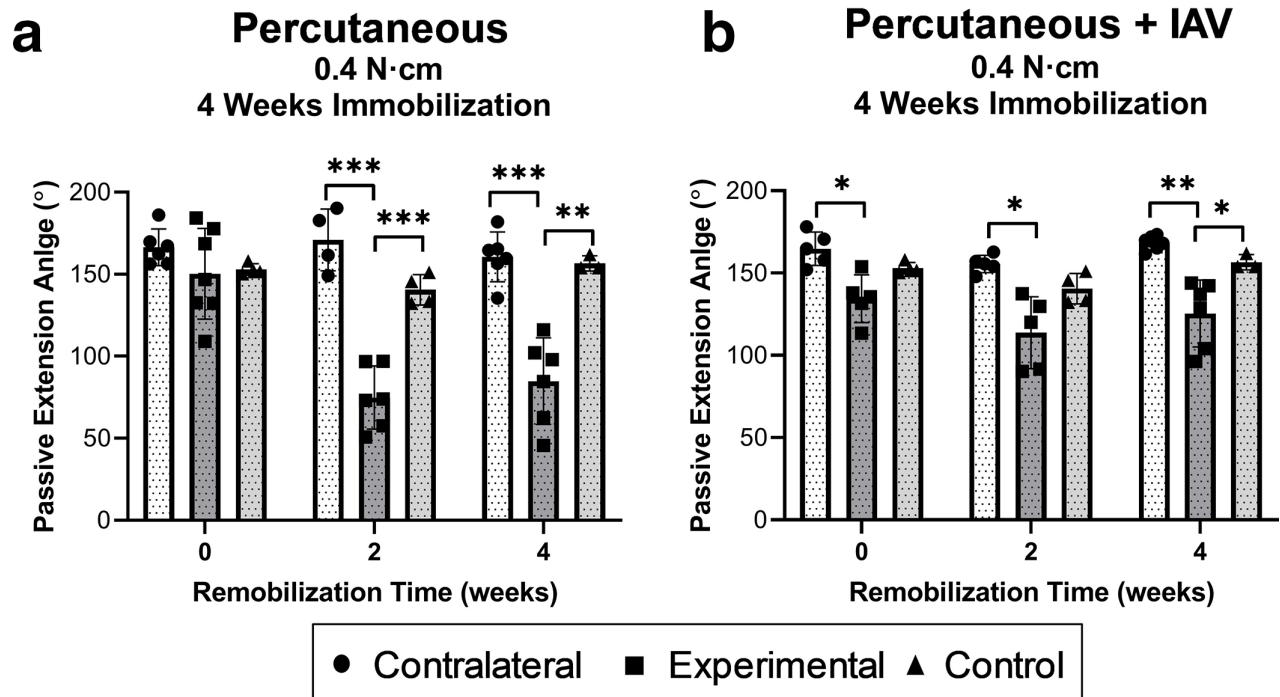
**Fig. 5**

Percutaneous and percutaneous + intra-articular violation methods induce knee stiffness after four weeks of immobilization. Biomechanical data after four weeks of immobilization showing passive extension angles registered at one specific torque (0.4 N-cm) and compared between experimental and contralateral knees from a) the percutaneous group and b) the percutaneous + intra-articular violation group. Individual mice are represented by a single point. Quantitative variables are reported as means and standard deviations. Significance is noted in the figures with a standard asterisk convention (*p ≤ 0.05, **p ≤ 0.01, ***p ≤ 0.001, ****p ≤ 0.0001). IAV, intra-articular violation.

single observer (LD) on a random selection of 10% of sections from each group (i.e. experimental, contralateral, and control limbs). Receiver operator characteristic (ROC) curve analysis was performed to evaluate the quantitative histological methods used. Threshold values were calculated using area under the curve (AUC). GraphPad Prism version 8.0.0 for Windows (GraphPad, USA) was used to perform all statistical analyses. A p-value < 0.05 was considered significant. No inclusion or exclusion criteria for experimental data were set.

## Results

**Surgical complications.** During the study period, six mice developed necrosis of the experimental foot during the first few days after surgery. This included one mouse from the eight-week immobilization/zero-week remobilization group, three mice from the eight-week immobilization/two-week remobilization group, and two mice from the eight-week immobilization/four-week remobilization group. These animals belonged to the percutaneous-only technique group during the first day of surgeries. Mice with necrotic feet were euthanized, as this was defined as a humane endpoint, and not replaced. An additional two mice experienced superficial wound infections and were successfully treated with local antibiotics.

**Biomechanical characterization.** To assess the extent of joint contracture after immobilization, mice were examined for biomechanical parameters after variable times of mobilization, remobilization, and endpoint analysis (Figure 1). The passive extension angle (PEA) was measured as the angle of displacement (e.g. straight knee was 180°) at 0.4 N-cm of torque.[24] After four weeks of immobilization with no remobilization, biomechanical testing revealed lower mean passive extension angles (PEAs) in the experimental knees (150° (SD 27.7°)) compared to the contralateral knees (166° (SD 11.1°)) in the percutaneous group (p = 0.3762, independent-samples t-test, Figure 5a). In addition, significant differences in PEAs were observed between experimental (134° (SD 14.5°)) and contralateral (164° (SD 10.2°)) knees after four weeks of immobilization and no remobilization in the percutaneous + intra-articular violation group (p = 0.015; Figure 5b, independent-samples t-test). As remobilization time increased, PEAs in the experimental knees were reduced when compared to contralateral knees for the percutaneous group (Figure 5a), with significant reductions in PEAs observed in the experimental knees after two weeks (75° (SD 19.2°) vs 171° (SD 18.9°), respectively; p = 0.003, independent-samples t-test) and four weeks (85° (SD 26.4°) vs 161° (SD 15.1°), respectively; p = 0.007, independent-samples t-test) of remobilization. Similar statistically significant trends were also observed when comparing experimental and contralateral knees in the percutaneous + intra-articular violation groups (Figure 5b).
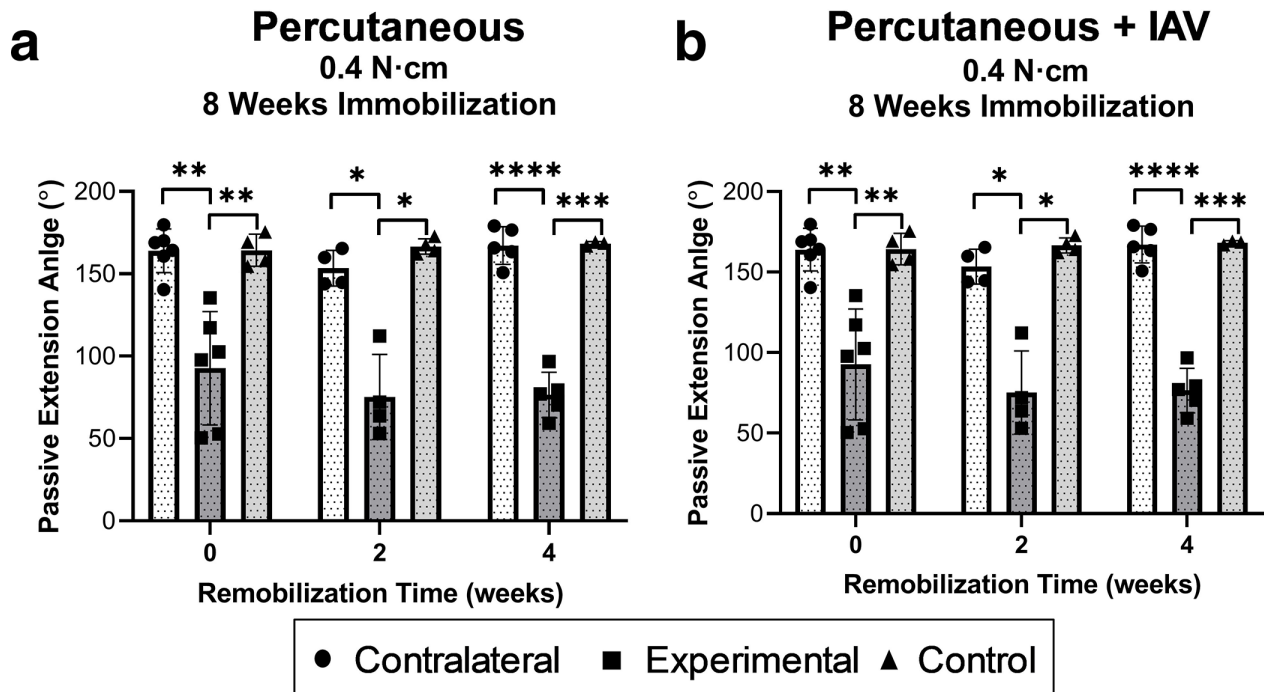
**a**
### Percutaneous
### 0.4 N·cm
### 8 Weeks Immobilization

**b**
### Percutaneous + IAV
### 0.4 N·cm
### 8 Weeks Immobilization



**Fig. 6**

Percutaneous and percutaneous + intra-articular violation methods induce persistent knee stiffness after eight weeks of immobilization. Biomechanical data after eight weeks of immobilization showing passive extension angles registered at one specific torques (0.4 N-cm) and compared between experimental and contralateral knees from a) the percutaneous group and b) the percutaneous + intra-articular violation group. Individual mice are represented by a single point. Quantitative variables are reported as means and standard deviations. Significance is noted in the figures with a standard asterisk convention (*p ≤ 0.05, **p ≤ 0.01, ***p ≤ 0.001, ****p ≤ 0.0001). IAV, intra-articular violation.

To understand the temporal impact of immobilization on joint contractures, we also analyzed mice that were immobilized for eight rather than four weeks (Figure 1). Mice with eight weeks of immobilization followed by zero weeks of remobilization demonstrated significantly reduced PEAs in experimental knees when compared to contralateral knees in the percutaneous group (93° (SD 34.5°) vs 164° (SD 13.2°), respectively; p = 0.006, independent-samples *t*-test; Figure 6a). Importantly, a reduction in PEAs of experimental knees was also observed in the percutaneous group in which remobilization was introduced for two weeks (75° (SD 25.8°) vs 153° (SD 10.8°), respectively; p = 0.011, independent-samples *t*-test) and four weeks (76° (SD 13.7°) vs 167° (SD 11.4°), respectively; p < 0.0001) following eight weeks of immobilization (Figure 6a). Similarly, significant reductions in the PEAs were also observed in the experimental knees when compared to contralateral knees in the percutaneous + intra-articular injury group after eight weeks of immobilization and followed by zero, two, and four weeks of remobilization (Figure 6b). In summary, these results demonstrate that both procedures, percutaneous and percutaneous + intra-articular violation, caused significant reductions in knee PEAs after weeks of immobilization. These findings also showed that induced contractures were robust, as knee PEAs did not improve in the experimental knees following remobilization. Importantly, our data also demonstrate that contralateral knees exhibited similar knee PEAs with control knees in non-surgical mice, irrespective of immobilization and remobilization periods (Figures 5 and 6).

To directly compare surgical methods, as well as temporal aspects of immobilization and remobilization, a comparison between experimental joints of percutaneous and percutaneous + intra-articular violation approaches across all immobilization and remobilization treatment periods was assessed (Figure 7). These additional analyses were performed using experimental knee data presented in Figures 5 and 6. While no differences were observed at four weeks following zero weeks of remobilization, the knee PEAs at four weeks of immobilization followed by two and four weeks of remobilization were non-significantly smaller in the percutaneous group when compared to the percutaneous + intra-articular violation group (Figure 7a). When similar comparisons were made for the eight-week immobilization groups, our analysis reveals similar knee PEAs after zero, two, and four weeks of remobilization between percutaneous and percutaneous + intra-articular violation groups (Figure 7b). Together, these data demonstrate that percutaneous and percutaneous + intra-articular violation approaches yielded similar knee stiffness phenotypes after an extensive immobilization period (i.e. eight weeks), while some differences are observed during shorter immobilization times (i.e. four weeks).
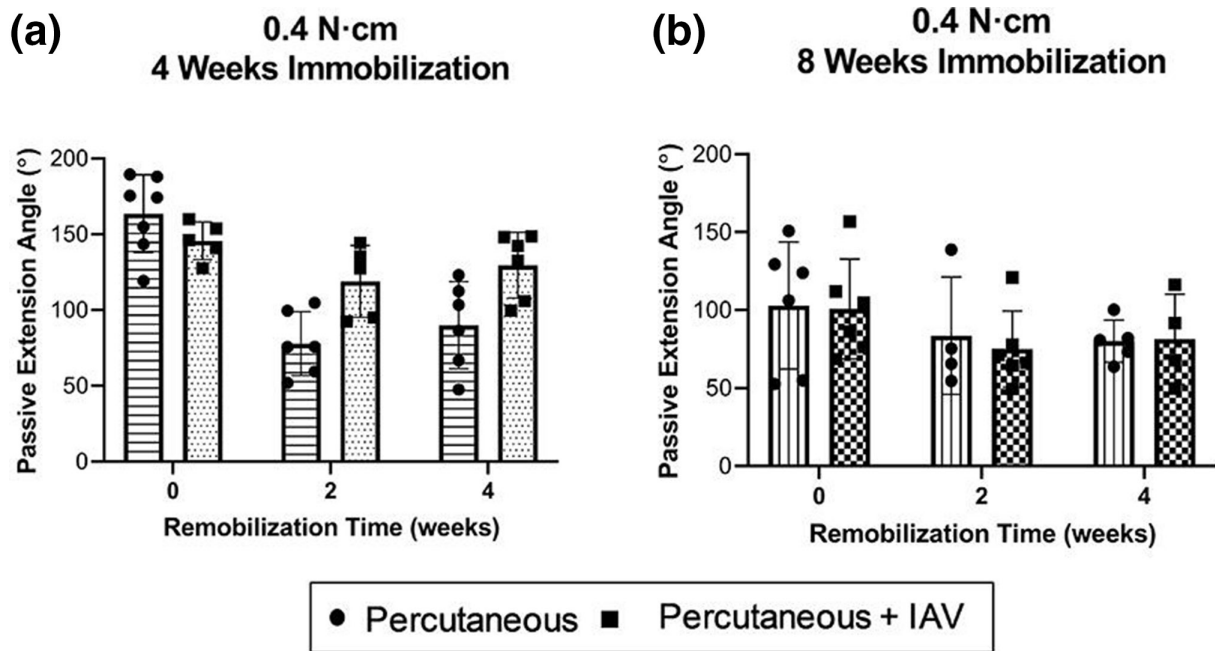
**Fig. 7**

Comparison of passive extension angles induced by percutaneous and percutaneous + intra-articular violation approaches. A direct comparison of biomechanical data after a) four weeks and b) eight weeks of immobilization of experimental knees from percutaneous and percutaneous + intra-articular violation groups registered at 0.4 N-cm torque. Of note, these experimental knee data are compared to contralateral and control knees in Figures 4 and 5. The experimental knee values are graphed again to allow for a comparison between percutaneous and percutaneous + intra-articular violation groups. Individual mice are represented by a single point. Quantitative variables are reported as means and standard deviations. Significance is noted in the figures with a standard asterisk convention (*p ≤ 0.05). IAV, intra-articular violation.

Collectively, biomechanical analyses reveal that a persistent contracture is generated after eight weeks of immobilization in both surgical techniques, and the remobilization period did not significantly increase knee PEAs. It is also worth noting that percutaneous and percutaneous + intra-articular violation approaches yield similar knee PEAs following eight weeks of immobilization, and contralateral knees exhibit similar knee flexion angles to control knees of naïve mice.

**Histological evaluation.** In addition to biomechanical studies, histological assessment was performed to examine capsular thickness and formation of periarticular connective tissue characteristic of joint contractures. The experimentation included semiquantitative analyses (i.e. subjective tissue characteristics applied to scoring criteria) and quantitative analyses (i.e. based on objective measurements). ICCs demonstrated good interobserver reliability and excellent intraobserver reliability for all methods (Table III).

Central sections of the knee showed significant differences in posterior capsular thickness after four weeks of immobilization in the percutaneous technique with four weeks of remobilization (100 μm (SD 23.3) in the experimental knees vs 44 μm (SD 4.9) in the contralateral knees; p = 0.043, independent-samples *t*-test) (Figure 8a, Table IV). No significant changes were observed in the percutaneous + intra-articular violation groups at four weeks of immobilization when compared

**Table III.** Reliability from our histological analysis.

| Variable | Intraobserver ICCs | Interobserver ICCs |
|---|---|---|
| Patellar tendon thickness (um) | 0.97 | 0.98 |
| Surface area anterior capsule (um^2) | 0.96 | 0.88 |
| Fibrotic tissue area - anterior capsule (um^2) | 0.78 | 0.56 |
| Ratio – anterior capsule (total SA/ fibrotic SA) | 0.82 | 0.72 |
| Posterior capsule thickness (um) | 0.92 | 0.95 |
| Surface area posterior capsule (um^2) | 0.94 | 0.91 |
| Fibrotic tissue area - posterior capsule (um^2) | 0.87 | 0.82 |
| Ratio - posterior capsule (total SA/ fibrotic SA) | 0.92 | 0.90 |

ICC, intraclass correlation coefficient; SA, surface area.

to the controls or contralateral knees, regardless of the remobilization period (Figure 8b, Table IV).

Central sections showed significant differences in the experimental knee joints when compared to contralateral and control knees after eight weeks of immobilization for all remobilization periods in the percutaneous approach (Figure 8c) as well as percutaneous + intra-articular

violation approach (Figure 8d). As an exception, the posterior capsule thickness was not different between contralateral and experimental knees at eight weeks following two weeks of remobilization (Figure 8c).

In addition to increased posterior capsular connective tissue deposition, increased deposition of connective tissue and thickness of the anterior infrapatellar tendon region was observed in the percutaneous technique after four weeks of immobilization and four weeks of remobilization between experimental knees versus contralateral knees (37 µm (SD 12.0) vs 15.5 µm (SD 10.7); p = 0.041, independent-samples *t*-test) and in the percutaneous + intra-articular violation technique after eight weeks of immobilization without remobilization between experimental stiff knees versus contralateral knees (39 µm (SD 4.0) vs 17 µm (SD 12.8); p = 0.020, independent-samples *t*-test) (Supplementary Figure a).

In addition to thickness of the anterior and posterior periarticular regions, the density of connective tissue was evaluated by comparing the total area of the region to the areas composed of non-connective tissue (i.e. adipose tissue); we defined this as the fibrotic ratio. Our data revealed that the fibrotic ratio (i.e. total area/fibrotic area) in the anterior compartment was significantly reduced in the percutaneous + intra-articular violation technique after four weeks of immobilization with two weeks of remobilization. The mean fibrotic ratio in the experimental stiff knees was 2.0 (SD 0.49), and significantly lower (i.e. increased percentage of fibrotic tissue) compared to the contralateral knees (3.8 (SD 0.55), p = 0.028, independent-samples *t*-test) and control knees (4.1 (SD 0.85), p = 0.037, independent-samples *t*-test), respectively (Supplementary Figure b).

Complementary to quantitative methods, qualitative methods were used to describe the capsular tissues and cartilage damage (Table II). The degree of arthrofibrosis was variable, with fibrotic and fatty infiltrate scores ranging from 0 to 2 in both techniques observed in the central sections. As such, increased fibrosis and reduced adiposity were observed in this mouse model for arthrofibrosis, corroborating the biological basis for the biomechanical outcomes that were measured.

In addition to the pericapsular tissue, cartilage was evaluated via toluidine blue staining and evaluated by a board certified veterinary histopathologist. The score used to assess the cartilage was a simplified version of a widely used OA scoring system.[29] Importantly, there was no cartilage damage observed via histological analysis in the percutaneous or percutaneous + intra-articular violation cohorts. All animals scored between 0 and 1 for cartilage damage, indicating that they had ≤ 10% of cartilage loss. The absence of cartilaginous injury was present regardless of the immobilization or remobilization period (Figure 9).

## Discussion

One major advantage of a mouse model over large animal models is the availability of knockout or transgenic mice to investigate the genetic mechanisms of fibrotic pathways.[13] In addition, there are many unique mouse strains and maintenance regimens that permit convenient modelling of comorbidities for arthrofibrosis. Therefore, the validation of a novel mouse model, dedicated to knee arthrofibrosis, is tremendously valuable.

We demonstrated that our surgical procedure, which involves limb immobilization via a loop around the femur and tibia using a nonabsorbable suture, generates a persistent contracture at four and eight weeks after surgery as assessed by biomechanical testing. The biomechanical alterations observed are supported by histological analysis, which revealed an increase in posterior capsule thickness after four and eight weeks of immobilization. These contractures are stable and persistent as remobilization did not alter PEAs. Together, our studies deliver a novel mouse model that is suitable for investigation of gene-specific functions and therapeutic-based approaches to identify candidate interventions in the treatment of arthrofibrosis.

The immobilization of one joint in a flexed position classically induces a flexion contracture.[20,30,31] In our model, mice developed an experimental knee contracture after the percutaneous fixation and was detectable via biomechanical analysis at four weeks after the index surgery. Similarly, Tokuda et al[20] demonstrated loss of motion in mice immobilized using external fixation for four weeks, however their study did not include any remobilization time to determine if the contracture was permanent. In addition, Nomura et al[23] examined hind limb unloading via tail suspension and hind limb fixation with Kirschner-wires in mice for two, four, and eight weeks, but also did not incorporate any remobilization time into their studies. Furthermore, they only examined the contracture formation with histological data, and did not show any biomechanical data. The contracture in our model was considered robust, as the remobilization periods (two and four weeks) analyzed in our study did not lead to spontaneous resolution of the contractures. However, at the time of removal surgery we did observe some callus formation over the suture at the femur-suture interface. The contracture appeared to mature during the remobilization period over the next few weeks even though the animals were remobilized. Similar biomechanical findings in a mouse model have only been reported in models that demonstrate significant cartilaginous damage as a result of contracture development.[14,15] Importantly, the biomechanical characteristics of the induced contracture were consistent with other validated animal models, including a rabbit model for arthrofibrosis[10–12] and another recently developed rat model of joint contracture.[7,24]

Conditions to immobilize the knee joint in animals are numerous, including external immobilization with tape,[20,21,32] joint compression,[33] suture fixation,[7] and metallic wire.[4,8,23,34,35] In choosing our method of immobilization, we were careful to balance the goals of the

## Percutaneous
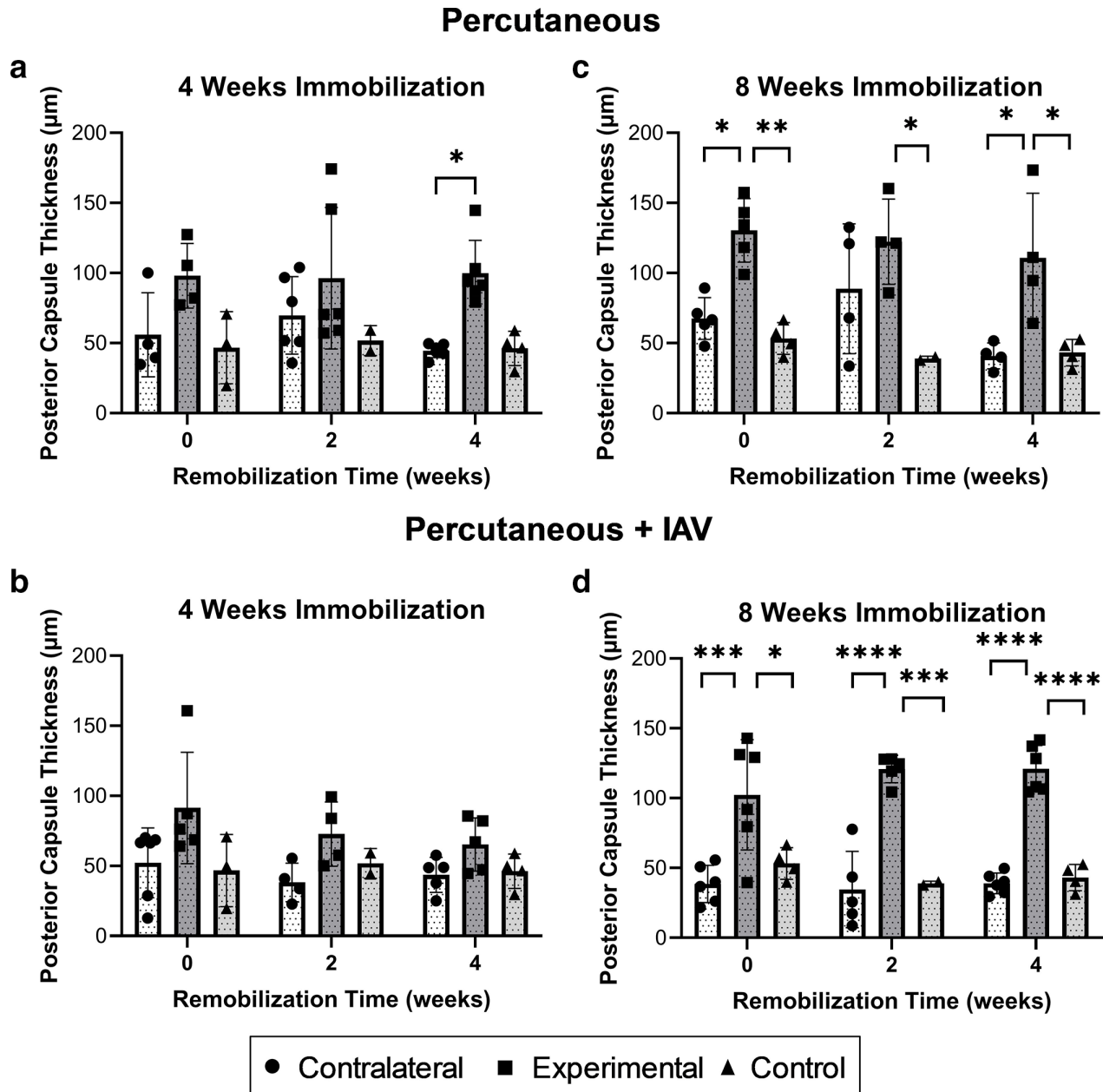


## Percutaneous + IAV

**Fig. 8**

Posterior capsule thickness is increased in the novel mouse model of arthrofibrosis. Posterior capsule thickness as measured by histology for experimental, contralateral, and control knees from the percutaneous group at a) four and c) eight weeks and percutaneous + intra-articular violation group at b) four and d) eight weeks. Individual mice are represented by a single point. Quantitative variables are reported as means and standard deviations. Significance is noted in the figures with a standard asterisk convention (*p ≤ 0.05, **p ≤ 0.01, ***p ≤ 0.001, ****p ≤ 0.0001). IAV, intra-articular violation.

procedures (contracture formation) versus unintended consequences (OA). To evaluate this aim, detailed histological analyses – both qualitative and quantitative – were used to evaluate the pericapsular tissue and cartilage. Importantly, the present model demonstrated increased fibrotic deposition in posterior capsular tissues without subsequent cartilaginous damage. These findings were analogous to those described in a rabbit model of arthrofibrosis.[11]

The present study establishes the first mouse model of arthrofibrosis that does not produce cartilage damage, although we acknowledge some similarities between our model and the rat model developed by Kallianos et al.[7] There are several levels of innovation in this mouse model. First, we performed a percutaneous technique to maintain the knee fixed during the study period. This technique provides high reproducibility, is relatively easy to learn and perform, and does

**Table IV.** Histological data after four weeks and eight weeks of immobilization, showing posterior capsule thickness in μm compared between contralateral, experimental stiff, and control knees from the percutaneous group and the percutaneous + intra-articular violation group.

| Surgical method | Immobilization time | Remobilization time | Mean posterior capsule thickness, μm (SD) | | | p-value | | |
|---|---|---|---|---|---|---|---|---|
| | | | Contra knees | Experimental knees | Control knees | Contra vs Experimental | Control vs Experimental | Control vs Contra |
| Percutaneous | 4 weeks | 0 weeks | 55.9 (30.0) | 98.1 (23.1) | 46.7 (25.7) | 0.487 | 0.330 | > 0.999 |
| | | 2 weeks | 69.8 (27.6) | 96.2 (50.5) | 51.8 (10.7) | 0.788 | 0.603 | 0.997 |
| | | 4 weeks | 44.6 (4.9) | 99.9 (23.3) | 46.2 (12.3) | 0.043* | 0.115 | > 0.999 |
| | 8 weeks | 0 weeks | 67.5 (14.9) | 130.4 (22.6) | 53.3 (11.3) | 0.023* | 0.006* | 0.996 |
| | | 2 weeks | 88.8 (46.3) | 122.3 (30.4) | 38.9 (1.7) | 0.702 | 0.030* | 0.466 |
| | | 4 weeks | 40.8 (9.3) | 110.8 (46.1) | 43.2 (9.4) | 0.024* | 0.032* | > 0.999 |
| Percutaneous + IAV | 4 weeks | 0 weeks | 52.2 (24.9) | 91.3 (39.8) | 46.7 (25.7) | 0.293 | 0.410 | > 0.999 |
| | | 2 weeks | 38.2 (13.7) | 72.7 (22.9) | 51.8 (10.7) | 0.028* | 0.037* | 0.999 |
| | | 4 weeks | 43.6 (12.5) | 65.3 (19.0) | 46.2 (12.3) | 0.026* | 0.869 | 0.577 |
| | 8 weeks | 0 weeks | 38.6 (13.3) | 102.4 (39.5) | 53.3 (11.3) | < 0.001* | 0.016* | 0.967 |
| | | 2 weeks | 34.6 (27.3) | 120.9 (9.9) | 38.9 (1.7) | < 0.001* | < 0.001* | > 0.999 |
| | | 4 weeks | 39.0 (7.5) | 121.1 (16.7) | 43.2 (9.4) | < 0.001* | < 0.001* | > 0.999 |

*Statistically significant.
Contra, contralateral; IAV, intra-articular violation.
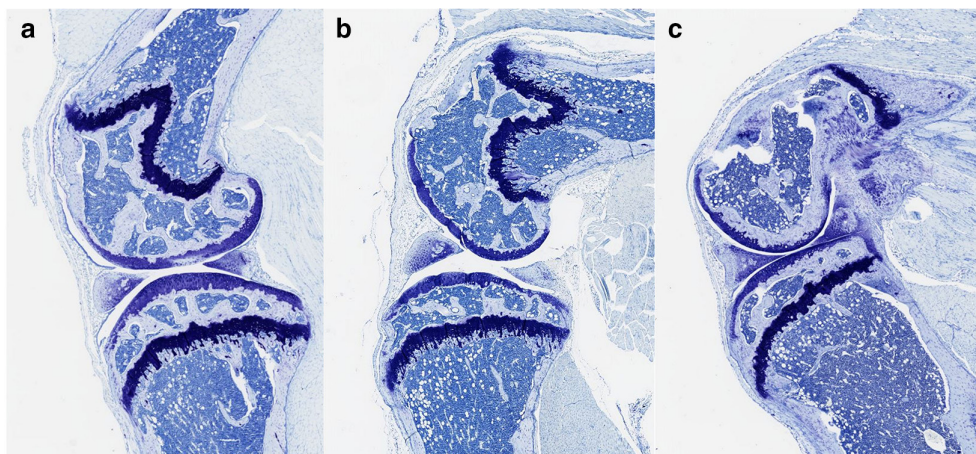


**Fig. 9**

No femoral and tibial osteoarthritic development in the novel mouse model shown using toluidine blue staining (20× magnification) between a) controls, and experimental knees at b) four weeks and c) eight weeks.

not involve high rates of complications. Additionally, contralateral limbs can be used as controls. We choose to not destabilize the knee joint using ligament disruption, as such techniques commonly induce OA-related synovial fibrosis.[22,36,37] Second, our study design allows for assessment of contracture duration after remobilization without comorbidities that are associated with destabilized knees, including post-traumatic OA.[22,36,37] The possibility for adding intra-articular injury (i.e. femoral condyle violation) allowed us to investigate the influence of intra-articular bleeding on the fibrotic pathway, which mimic the conventional process after orthopaedic surgery. However, this additional manipulation had minimal effects on the overall phenotype. As such, the percutaneous technique may be more appropriate going forward as it allows fewer surgical steps

without major differences in biomechanical and histological properties.

While numerous advantages exist, some limitations to our model, specifically regarding the surgical technique, need to be discussed. First, it is possible that the suture may slide along the femur and the tibia, especially during weightbearing, and alter range of motion of the knee. The suture was placed on the proximal end of the femoral bow and the distal end of the tibia bow, which should have limited the motion of the knotted suture. In support, the location of the suture at removal surgery matched the placement location of the suture at the time of index surgery. Also, we did not observe any instances of the suture sliding off the femur or tibia. Importantly, with the exception of the four weeks of immobilization and 0 weeks of immobilization group,

which may have been confounded by a learning curve (discussed below), the biomechanical data clustered together for each group, suggesting that each animal exhibited similar contractures during each timepoint. Second, it is possible that the passing of the needle and/or the tightening of the suture could cause damage/compression to the surrounding bones or soft-tissues, which could in turn contribute to the contracture formation. Although we only observed some callus formation on the femur at the suture placement site, we were not able to assess the soft-tissue for any damage after the passing or tightening of the suture. Third, the results of the groups with four weeks of immobilization and 0 weeks of remobilization were possibly confounded due to the learning curve of the technique during this time, as these were the first surgeries performed. It was important to the authors to ratify this data, which was recently done as part of another project (Supplementary Figure c). Moreover, even with the addition of these data, the biomechanical and histological data proved to have less variation with eight weeks of immobilization. Thus, future studies using this model may benefit from immobilization periods that are longer than four weeks, to reduce variation and number of animals required for each group for proper statistical assessment. Fourth, the intra-articular injury to the joint may not have been sufficient to induce a haematoma. Other options need to be explored for creating this injury to the joint.

Some additional limitations of our study overall are, first, that it only included female mice. This decision was made to promote homogeneity among size and weight of the cohort. Female mice were preferred because the authors acknowledge that there are sex differences in the pathogenesis of arthrofibrosis[2] and cartilage degeneration in humans.[38] However, similar to sex-dependent differences observed in the destabilization of the medial meniscus to induce OA in mice,[39] the possibility exists that male and female mice may respond differently in our knee immobilization model. Second, mice were operated on before skeletal maturity, which usually occurs around 16 to 18 weeks of age.[40] As such, later stages in skeletal maturity can interact with cartilage degeneration, since delayed chondrocyte maturation is less susceptible to developing OA in mice.[41] Third, our design cannot accurately determine the specific effect of extra-articular or intra-articular dimensions of the knee contracture. Evaluation of the joint via 3D imaging (i.e. MRI[42] or molecular approaches (e.g. RNA expression) would provide enhanced understanding of the architecture of periarticular fibrosis in mice. Furthermore, these additional findings could then be compared to arthrofibrotic human tissues and established animal models of arthrofibrosis. Fourth, the histological measurements of the posterior and anterior capsules could be influenced by the flexion angle of the embedded knee. This is something that will need to be addressed in future studies. Fifth, we did not access cartilage thickness. Other studies have demonstrated cartilage thinning

with knee immobilization.[23] This will be an important area of examination for future studies. Sixth, this study examined the extension deficit of the operative limbs induced by suture immobilization in knee flexion, and results may not represent arthrofibrotic phenotypes related to stiffness in flexion, which require extension immobilization and specific methodology.

In summary, this study delivers a versatile and validated mouse model of arthrofibrosis that avoids cartilage damage. The contractures that are generated are robust, and are not resolved by variable periods of remobilization. This relative permanence provides a robust experimental endpoint that can then be improved upon by therapeutic strategies to reduce or reverse joint contracture. This mouse model of arthrofibrosis may be employed in future studies to define molecular mechanisms that regulate joint stiffness, and assess the utility of pharmacological interventions in the treatment of arthrofibrosis.

## Supplementary material

ë Figures illustrating data for the other histological measurements performed for this study, and biomechanical data from a different experiment shown to validate the four-week immobilization with zero weeks of remobilization timepoint. An ARRIVE checklist is also included to show that the ARRIVE guidelines were adhered to in this study.

## References

1. **Ibrahim IO**, **Nazarian A**, **Rodriguez EK**. Clinical management of arthrofibrosis: State of the art and therapeutic outlook. *JBJS Rev*. 2020;8(7):e1900223.
2. **Tibbo ME**, **Limberg AK**, **Salib CG**, **et al**. Acquired idiopathic stiffness after total knee arthroplasty: A systematic review and meta-analysis. *J Bone Joint Surg Am*. 2019;101-A(14):1320–1330.
3. **Dagneaux L**, **Owen AR**, **Bettencourt JW**, **et al**. Human fibrosis: Is there evidence for a genetic predisposition in musculoskeletal tissues? *J Arthroplasty*. 2020;35(11):3343–3352.
4. **Nesterenko S**, **Morrey ME**, **Abdel MP**, **et al**. New rabbit knee model of posttraumatic joint contracture: indirect capsular damage induces a severe contracture. *J Orthop Res*. 2009;27(8):1028–1032.
5. **Abdel MP**, **Morrey ME**, **Barlow JD**, **et al**. Myofibroblast cells are preferentially expressed early in a rabbit model of joint contracture. *J Orthop Res*. 2012;30(5):713–719.
6. **Morrey ME**, **Abdel MP**, **Riester SM**, **et al**. Molecular landscape of arthrofibrosis: Microarray and bioinformatic analysis of the temporal expression of 380 genes during contracture genesis. *Gene*. 2017;610:15–23.
7. **Kallianos SA**, **Singh V**, **Henry DS**, **Berkoff DJ**, **Arendale CR**, **Weinhold PS**. Interleukin-1 receptor antagonist inhibits arthrofibrosis in a post-traumatic knee immobilization model. *Knee*. 2021;33:210–215.
8. **Arsoy D**, **Salib CG**, **Trousdale WH**, **et al**. Joint contracture is reduced by intra-articular implantation of rosiglitazone-loaded hydrogels in a rabbit model of arthrofibrosis. *J Orthop Res*. 2018;36(11):2949–2955.
9. **Barlow JD**, **Morrey ME**, **Hartzler RU**, **et al**. Effectiveness of rosiglitazone in reducing flexion contracture in a rabbit model of arthrofibrosis with surgical capsular release: A biomechanical, histological, and genetic analysis. *Bone Joint Res*. 2016;5(1):11–17.
10. **Limberg AK**, **Tibbo ME**, **Salib CG**, **et al**. Reduction of arthrofibrosis utilizing a collagen membrane drug-eluting scaffold with celecoxib and subcutaneous injections with ketotifen. *J Orthop Res*. 2020;38(11):2474–2483.
11. **Salib CG**, **Reina N**, **Trousdale WH**, **et al**. Inhibition of COX-2 pathway as a potential prophylaxis against arthrofibrogenesis in a rabbit model of joint contracture. *J Orthop Res*. 2019;37(12):2609–2620.

12. **Tibbo ME**, **Limberg AK**, **Salib CG**, **et al**. Anti-fibrotic effects of the antihistamine ketotifen in a rabbit model of arthrofibrosis. *Bone Joint Res*. 2020;9(6):302–310.

13. **Lorenz J**, **Grässel S**. Experimental osteoarthritis models in mice. *Methods Mol Biol*. 2014;1194:401–419.

14. **Culley KL**, **Singh P**, **Lessard S**, **et al**. Mouse models of osteoarthritis: surgical model of post-traumatic osteoarthritis induced by destabilization of the medial meniscus. *Methods Mol Biol*. 2021;2221:223–260.

15. **Hsia AW**, **Anderson MJ**, **Heffner MA**, **Lagmay EP**, **Zavodovskaya R**, **Christiansen BA**. Osteophyte formation after ACL rupture in mice is associated with joint restabilization and loss of range of motion. *J Orthop Res*. 2017;35(3):466–473.

16. **Li J**, **Anemaet W**, **Diaz MA**, **et al**. Knockout of ADAMTS5 does not eliminate cartilage aggrecanase activity but abrogates joint fibrosis and promotes cartilage aggrecan deposition in murine osteoarthritis models. *J Orthop Res*. 2011;29(4):516–522.

17. **Watson RS**, **Gouze E**, **Levings PP**, **et al**. Gene delivery of TGF-$\beta$1 induces arthrofibrosis and chondrometaplasia of synovium in vivo. *Lab Invest*. 2010;90(11):1615–1627.

18. **van Beuningen HM**, **Glansbeek HL**, **van der Kraan PM**, **van den Berg WB**. Osteoarthritis-like changes in the murine knee joint resulting from intra-articular transforming growth factor-beta injections. *Osteoarthritis Cartilage*. 2000;8(1):25–33.

19. **National Research Council Committee for the Update of the Guide for the C, Use of Laboratory A**. *The National Academies Collection: Reports funded by National Institutes of Health. Guide for the Care and Use of Laboratory Animals*. Washington, (DC): National Academies Press (US), 2011.

20. **Tokuda K**, **Yamanaka Y**, **Kosugi K**, **et al**. Development of a novel knee contracture mouse model by immobilization using external fixation. *Connect Tissue Res*. 2022;63(2):169–182.

21. **Tokuda K**, **Yamanaka Y**, **Mano Y**, **et al**. Effect of metformin treatment and its time of administration on joint capsular fibrosis induced by mouse knee immobilization. *Sci Rep*. 2021;11(1):17978.

22. **Rai MF**, **Duan X**, **Quirk JD**, **et al**. Post-traumatic osteoarthritis in mice following mechanical injury to the synovial joint. *Sci Rep*. 2017;7:45223.

23. **Nomura M**, **Sakitani N**, **Iwasawa H**, **et al**. Thinning of articular cartilage after joint unloading or immobilization. An experimental investigation of the pathogenesis in mice. *Osteoarthritis Cartilage*. 2017;25(5):727–736.

24. **Owen AR**, **Dagneaux L**, **Limberg AK**, **et al**. Biomechanical, histological, and molecular characterization of a new posttraumatic model of arthrofibrosis in rats. *J Orthop Res*. 2022;40(2):323–337.

25. **Swan KG**, **Baldini T**, **McCarty EC**. Arthroscopic suture material and knot type: an updated biomechanical analysis. *Am J Sports Med*. 2009;37(8):1578–1585.

26. **Reina N**, **Trousdale WH**, **Salib CG**, **et al**. Validation of a dynamic joint contracture measuring device in a live rabbit model of arthrofibrosis. *J Orthop Res*. 2018.

27. **Watanabe M**, **Kojima S**, **Hoso M**. Effect of low-intensity pulsed ultrasound therapy on a rat knee joint contracture model. *J Phys Ther Sci*. 2017;29(9):1567–1572.

28. **Eliasziw M**, **Young SL**, **Woodbury MG**, **Fryday-Field K**. Statistical methodology for the concurrent assessment of interrater and intrarater reliability: using goniometric measurements as an example. *Phys Ther*. 1994;74(8):777–788.

29. **Glasson SS**, **Chambers MG**, **Van Den Berg WB**, **Little CB**. The OARSI histopathology initiative - recommendations for histological assessments of osteoarthritis in the mouse. *Osteoarthritis Cartilage*. 2010;18 Suppl 3:S17–23.

30. **Baranowski A**, **Schlemmer L**, **Förster K**, **et al**. A novel rat model of stable posttraumatic joint stiffness of the knee. *J Orthop Surg Res*. 2018;13(1):185.

31. **Dunham CL**, **Castile RM**, **Chamberlain AM**, **Lake SP**. The role of periarticular soft tissues in persistent motion loss in a rat model of posttraumatic elbow contracture. *J Bone Joint Surg Am*. 2019;101-A(5):e17.

32. **Sotobayashi D**, **Kawahata H**, **Anada N**, **Ogihara T**, **Morishita R**, **Aoki M**. Therapeutic effect of intra-articular injection of ribbon-type decoy oligonucleotides for hypoxia inducible factor-1 on joint contracture in an immobilized knee animal model. *J Gene Med*. 2016;18(8):180–192.

33. **Wong K**, **Trudel G**, **Laneuville O**. Noninflammatory joint contractures arising from immobility: Animal models to future treatments. *Biomed Res Int*. 2015;2015:848290.

34. **Abdel MP**, **Morrey ME**, **Barlow JD**, **et al**. Intra-articular decorin influences the fibrosis genetic expression profile in a rabbit model of joint contracture. *Bone Joint Res*. 2014;3(3):82–88.

35. **Abdel MP**, **Morrey ME**, **Grill DE**, **et al**. Effects of joint contracture on the contralateral unoperated limb in a rabbit knee contracture model: a biomechanical and genetic study. *J Orthop Res*. 2012;30(10):1581–1585.

36. **Brown SB**, **Hornyak JA**, **Jungels RR**, **et al**. Characterization of post-traumatic osteoarthritis in rats following anterior cruciate ligament rupture by non-invasive knee injury (NIKI). *J Orthop Res*. 2020;38(2):356–367.

37. **Pragnère S**, **Boulocher C**, **Pollet O**, **et al**. Mechanical alterations of the bone-cartilage unit in a rabbit model of early osteoarthrosis. *J Mech Behav Biomed Mater*. 2018;83:1–8.

38. **Ro JY**, **Zhang Y**, **Tricou C**, **Yang D**, **da Silva JT**, **Zhang R**. Age and sex differences in acute and osteoarthritis-like pain responses in rats. *J Gerontol A Biol Sci Med Sci*. 2020;75(8):1465–1472.

39. **Hwang HS**, **Park IY**, **Hong JI**, **Kim JR**, **Kim HA**. Comparison of joint degeneration and pain in male and female mice in DMM model of osteoarthritis. *Osteoarthritis Cartilage*. 2021;29(5):728–738.

40. **Almeida M**, **O'Brien CA**. Basic biology of skeletal aging: role of stress response pathways. *J Gerontol A Biol Sci Med Sci*. 2013;68(10):1197–1208.

41. **Lu Y**, **Ding M**, **Li N**, **et al**. Col10a1-Runx2 transgenic mice with delayed chondrocyte maturation are less susceptible to developing osteoarthritis. *Am J Transl Res*. 2014;6(6):736–745.

42. **Attard V**, **Li CY**, **Self A**, **et al**. Quantification of intra-articular fibrosis in patients with stiff knee arthroplasties using metal-reduction MRI. *Bone Joint J*. 2020;102-B(10):1331–1340.

**Author information:**
- L. Dagneaux, MD, Orthopaedic Surgeon
- A. K. Limberg, BS, Scientist
- A. R. Owen, MD, Orthopaedic Surgeon
- J. W. Bettencourt, BS, Scientist
- A. Dudakovic, PhD, Scientist
- B. Bayram, PhD, Scientist
- J. Sanchez-Sotelo, MD, PhD, Orthopaedic Surgeon
- D. J. Berry, MD, Orthopaedic Surgeon, Head of Department
- M. E. Morrey, MD, Orthopaedic Surgeon
- M. P. Abdel, MD, Orthopaedic Surgeon, Principal Investigator
  Department of Orthopedic Surgery, Mayo Clinic, Rochester, Minnesota, USA.
- N. M. Gades, DVM, MS, Pathologist, Department of Comparative Medicine, Mayo Clinic, Scottsdale, Arizona, USA.
- A. van Wijnen, PhD, Scientist, Department of Orthopedic Surgery, Mayo Clinic, Rochester, Minnesota, USA; Department of Biochemistry, University of Vermont, Burlington, Vermont, USA.